

Supporting Information

Unified Film Patterning and Annealing of an Organic Semiconductor with Micro-Grooved Wet Stamps

Kyunghun Kim^{1,‡}, Mi Jang^{2,‡}, Minjung Lee², Tae Kyu An³, John E. Anthony⁴, Se Hyun Kim^{5,},
Hoichang Yang^{2,*}, and Chan Eon Park^{1,*}*

¹Department of Chemical Engineering, Pohang University of Science and Technology, Pohang
790-784, Korea

²Department of Applied Organic Materials Engineering, Inha University, Incheon 402-751,
Korea

³Department of Polymer Science and Engineering, Korea National University of
Transportation, Chungju, 27469, Korea

⁴Department of Chemistry, University of Kentucky, Kentucky 40506, USA

⁵Division of Chemical Engineering, Yeungnam University, Gyeongsan 712-749, Korea

KEYWORDS: direct solvent annealing; triethylsilylethynyl-anthradithiophene (TES-ADT);
soft patterning; uniformity; organic field-effect transistor

‡K.K. and M.J. contributed equally to this work.

*Corresponding authors: hcyang@inha.ac.kr; cep@postech.ac.kr; shkim97@yu.ac.kr

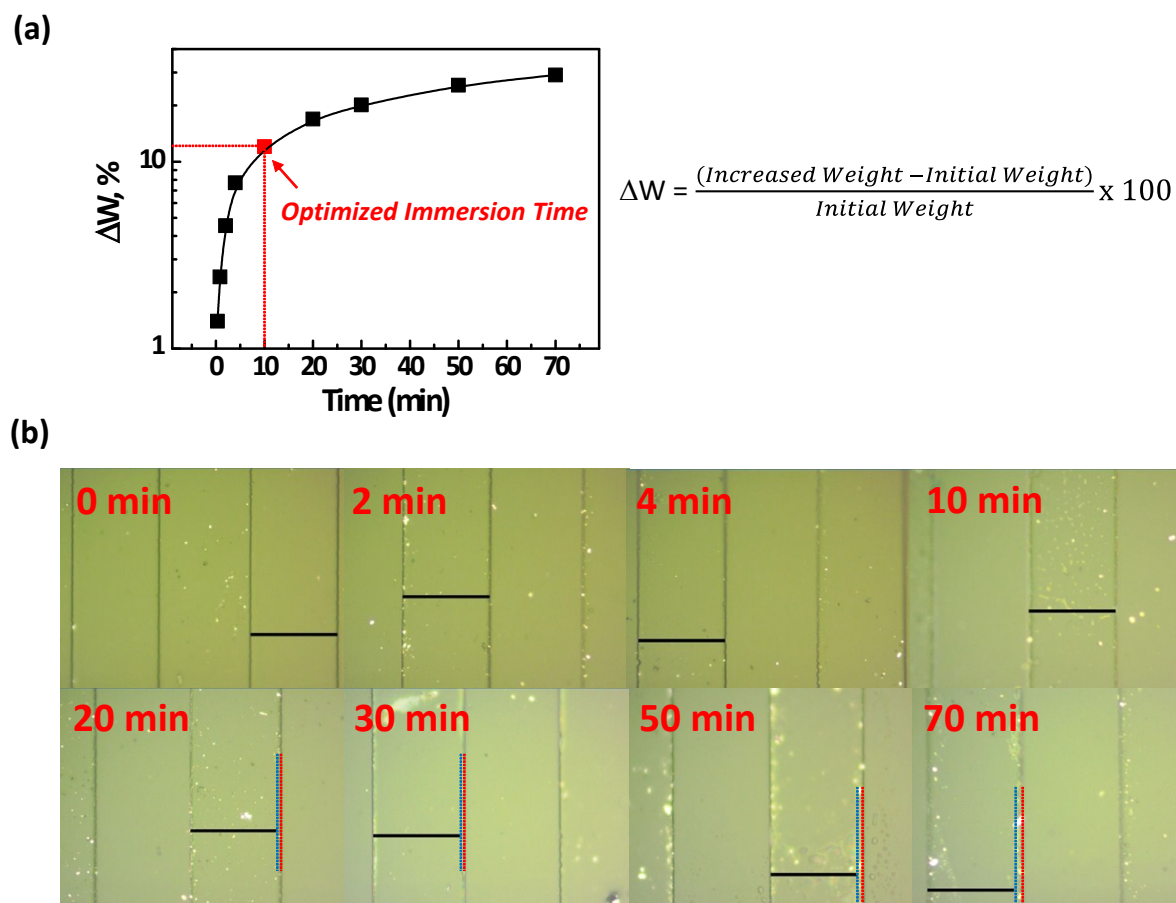


Figure S1. (a) Degree of weight increase and (b) OM images of the 50 μm -patterned PDMS stamp over time during immersion in the DCE reservoir. Note that in (b), the black scale bars indicate 50 μm . As the immersion time increased, particularly after 10 min, the line width of the PDMS stamp increase, indicating swelling in the PDMS.

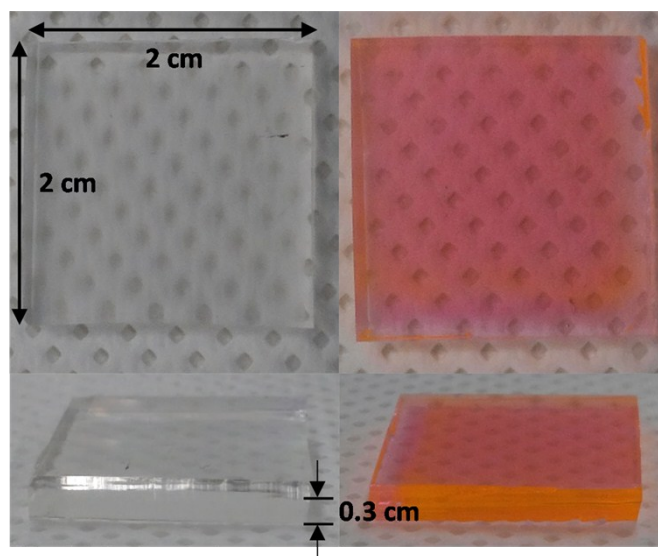


Figure S2. Photographs of the μ -PDMS stamps before and after the TES-ADT patterning process.

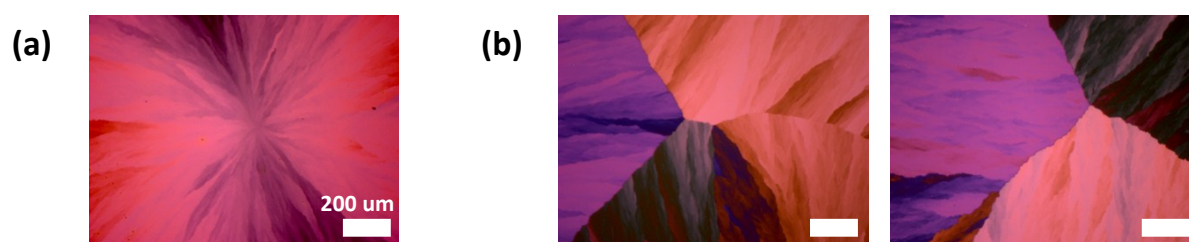


Figure S3. Polarized OM images of the unpatterned TES-ADT films after applying the solvent annealing process.

(a) The radial growth of TES-ADT crystals from the nucleation site, and (b) the impingement among crystallites grown from different nucleation sites.

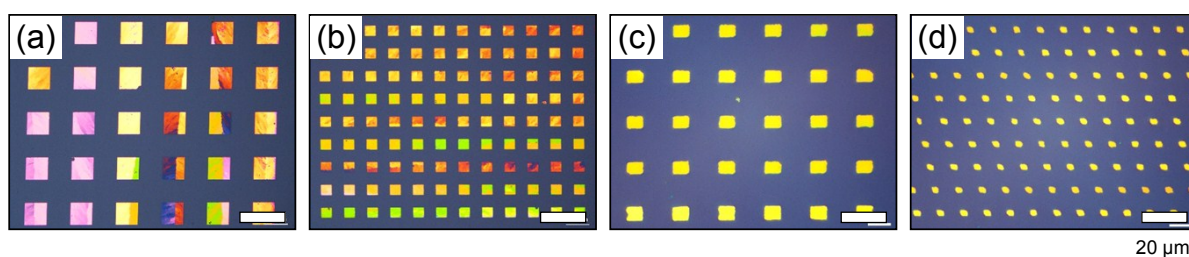


Figure S4. Polarized OM images of square-patterned TES-ADT films prepared using (a) 100, (b) 50, (c) 10, (d) $2.5 \mu\text{m}$ line patterned PDMS stamps.

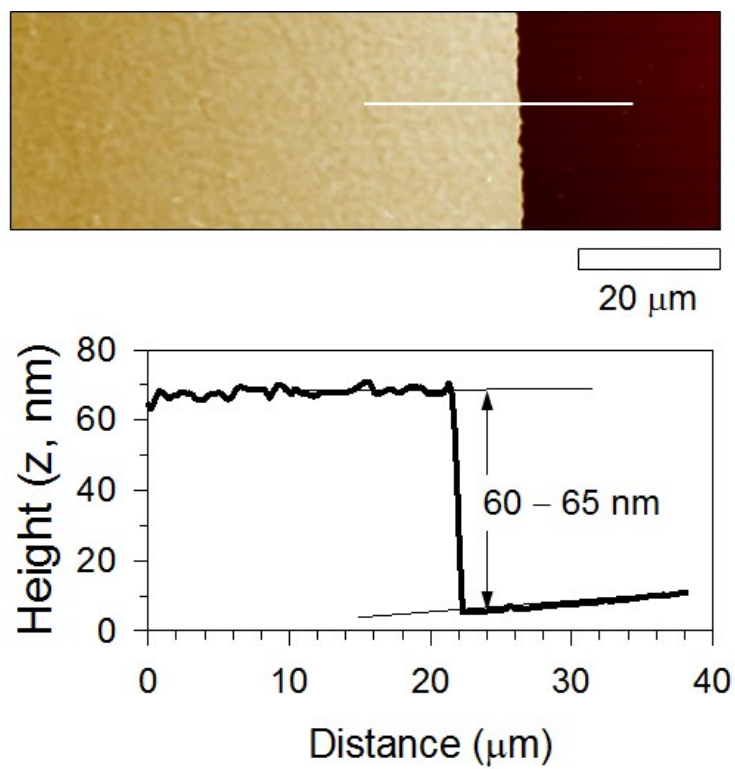


Figure S5. AFM topography (top) and cross-section profile (bottom) of the 100- μm patterned TES-ADT film.

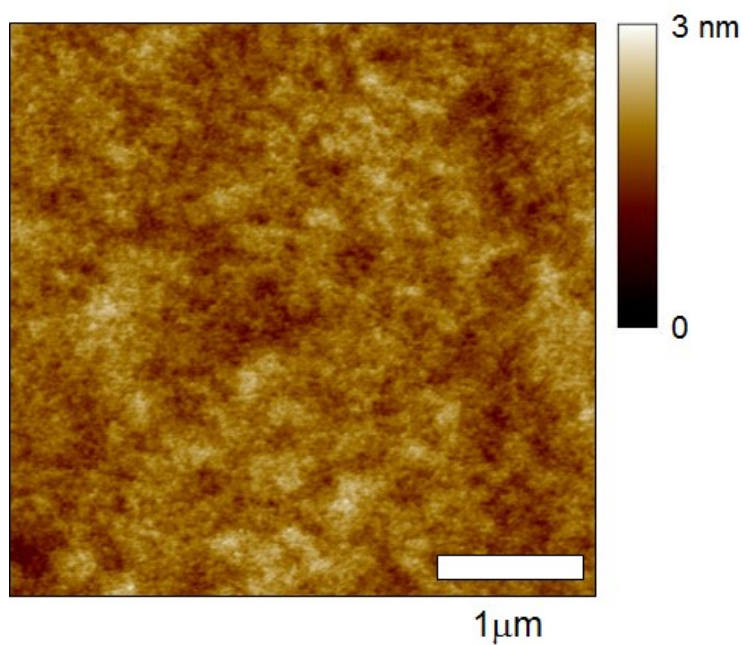


Figure S6. 2 μm \times 2 μm AFM topography image of the as-spun TES-ADT film.

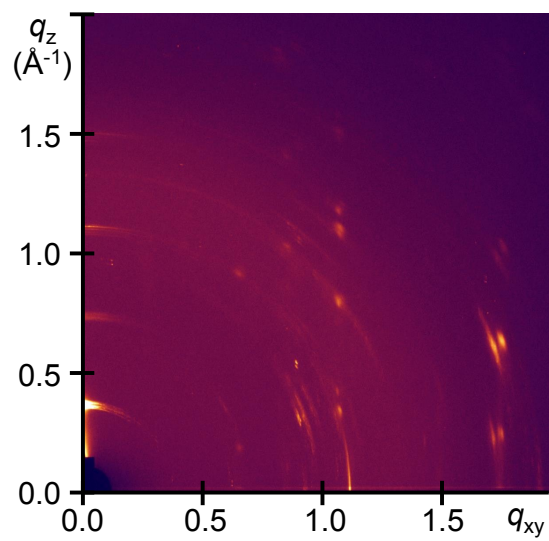


Figure S7. 2D GIXD patterns of the as-spun TES-ADT film.

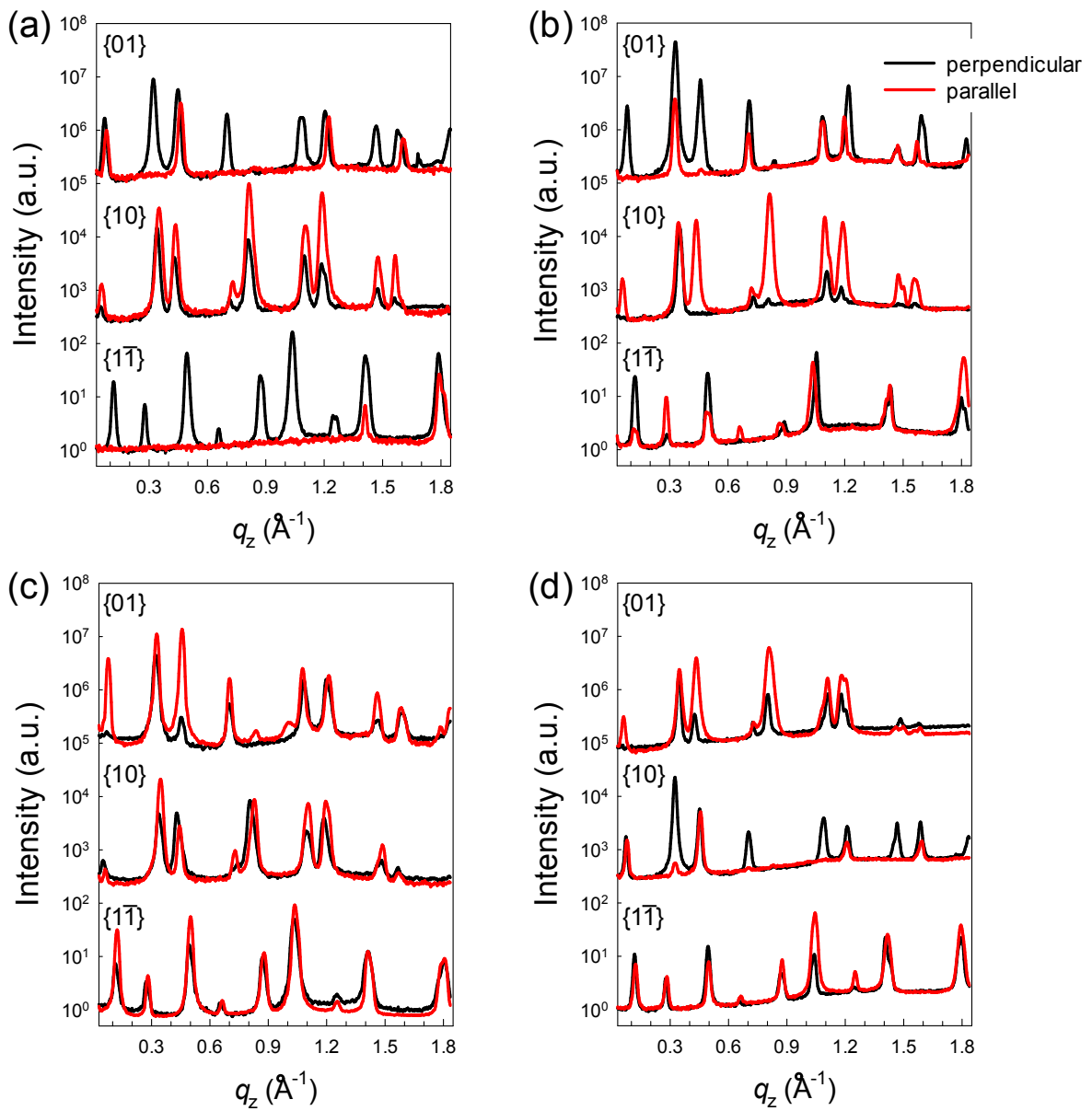


Figure S8. 1D X-ray reflections extracted at $q_{\{01\}}$, $q_{\{10\}}$, and $q_{\{1\bar{1}\}}$ from the 2D GIXD patterns of (a) 100, (b) 50, (c) 10, (d) 2.5 μm TES-ADT samples (Figure 5).

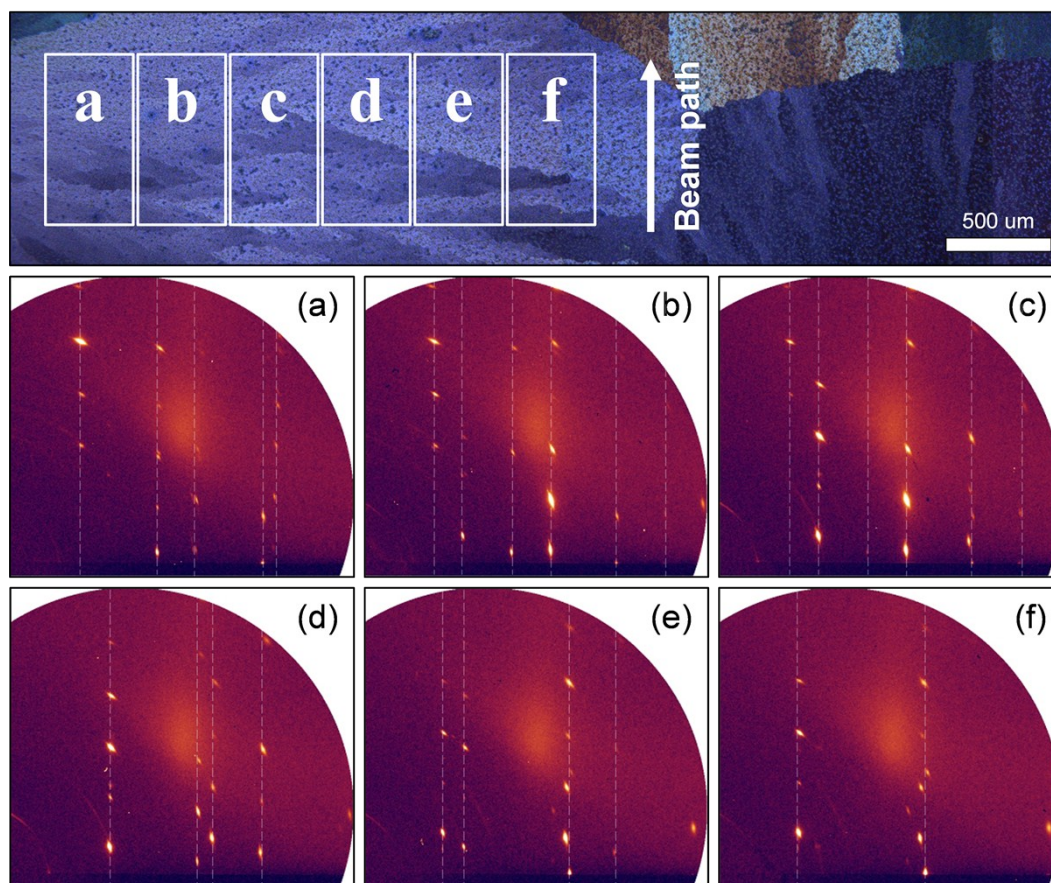


Figure S9. 2D GIXD patterns obtained from a normal DSA-treated TES-ADT film along the footprint of the incident beam with a width \times height of $300 \times 50 \mu\text{m}^2$. The patterns corresponding to each footprint are indicated in the upward-polarized OM images.

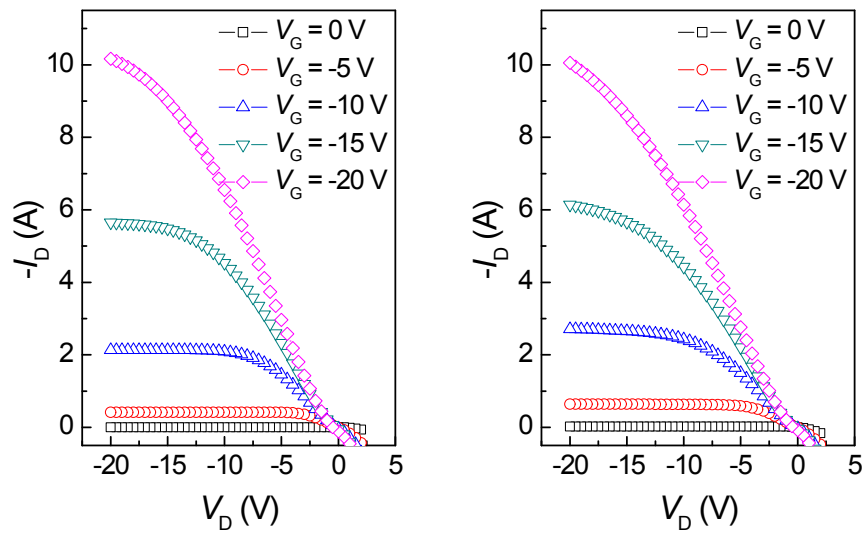


Figure S10. Output characteristics of OFETs prepared with 100 or 2.5 μm -patterned TES-ADT film.